World Journal of Biology Pharmacy and Health Sciences
eISSN: 2582-5542
Cross Ref DOI: 10.30574/wjbphs
Journal homepage: https://wjbphs.com/

(REVIEW ARTICLE)

Check for updates

THE EVOLUTION AND PARADIGMS OF DIAGNOSTIC MICROBIOLOGY

Juan Pablo Domínguez Enríquez [1,*] and Cristian David Cusco Cuzco [2]

[1] Pontificia Universidad Católica de Quito, Faculty of medicine Quito, Ecuador.
[2] Medical department, Oasis of the Seas, Royal CaCG, Miami USA.
* Corresponding Author

ORCID Details
Juan Pablo Domínguez Enríquez: https://orcid.org/0000-0002-1120-3335

World Journal of Biology Pharmacy and Health Sciences, 2026, 28(01), 026–035

Publication history: Received on 10 August 2026; revised on 29 September 2026; accepted on 01 October 2026

Article DOI: https://doi.org/10.30574/wjbphs.2026.28.1.0489

Copyright © 2026 Author(s) retain the copyright of this article. This article is published under the terms of the Creative Commons Attribution License 4.0

ABSTRACT

Diagnostic microbiology has evolved from early observational microscopy to advanced molecular, biochemical, and immunodiagnostic methodologies. This article traces the historical evolution and development of microbiological diagnostic techniques. Key methods examined include light microscopy, differential staining (such as Gram and acid-fast stains), solid culture media, colorimetric metabolic profiling (API 20E), and immunodiagnostic serotyping. Finally, we analyze the role of modern genomic tools specifically 16S ribosomal RNA (rRNA) gene sequencing and phylogenetic reconstruction in establishing a definitive microbial taxonomy. Together, these complementary paradigms form the foundation of contemporary clinical diagnosis.

Keywords: Diagnostic Microbiology, Gram Stain, Acid-Fast Stain, Nugent Score, API 20E, Immunodiagnostics, 16S Rrna Sequencing, Phylogenetics.

1 INTRODUCTION

Microbiological diagnosis is a multi-stage process essential for the confirmation and definitive identification of human pathogens. Historically, microscopy served as the cornerstone that dismantled dogmatic paradigms, mystical explanations, and the miasma theory that attributed infections to foul air or putrid vapors, thereby paving the way for identifying the true etiologic agents of disease. Prior to its consolidation, concepts regarding the origin of disease oscillated between supernatural beliefs and Galenic traditions inherited from antiquity. This paradigm began to shift in 1665 when Robert Hooke, utilizing an early compound microscope, documented microfungi (Mucor) and first described the cell as a biological unit in his treatise Micrographia [Fig. 1], published by the Royal Society [1]. Shortly thereafter, in 1676, the Dutch naturalist Antonie van Leeuwenhoek employed single-lens simple microscopes estimated to magnify roughly 70× to 250× with unprecedented optical precision to describe the first living microorganisms, which he famously termed "animalcules," now recognized as bacteria and protozoa; this body of work established him as the "Father of Microbiology" [1][2][3][4]. Notably, neutron tomography of van Leeuwenhoek's surviving instruments has shown that his best-performing microscopes incorporated a lens-making procedure popularized by Hooke, indicating the two were less independent than traditionally portrayed [2].

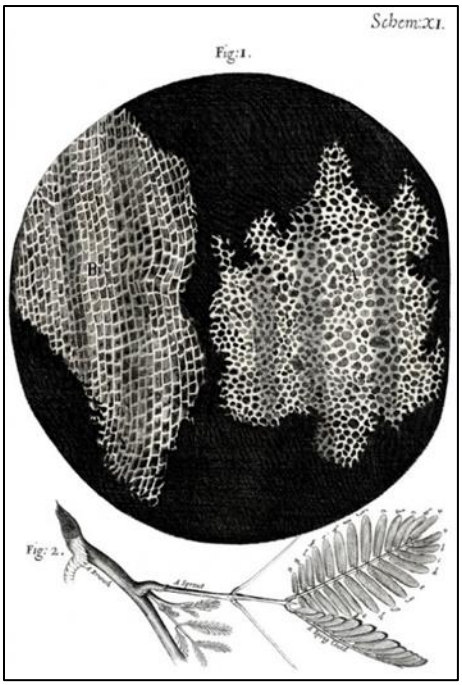


Figure 1. Historical illustrations from Robert Hooke's seminal 1665 work

Note: *Micrographia*, depicting (a) his compound microscope and (b) the cork cell structures he observed.

Despite these groundbreaking observations, seventeenth- and early eighteenth-century microscopy faced severe technical limitations. Optical aberrations and a lack of specimen contrast prevented the visualization of internal morphological features and the differentiation of clinically relevant species. It was not until the second half of the nineteenth century, within the framework of the germ theory of disease, that advances in modern optics, such as Ernst Abbe's oil immersion objectives, converged with the development of solid culture media and biological staining techniques to revolutionize diagnostic microbiology [16].

2 CULTURE MEDIA AND PHENOTYPIC CHARACTERIZATION

Parallel to optical advancements, the development of solid culture media transformed the field, largely due to the decisive contribution of Fanny Hesse and her husband, Walther Hesse, working in Robert Koch’s laboratory. Fanny Hesse proposed using agar-agar as a solidifying agent, allowing media to remain stable at human incubation temperatures and unlocking vast possibilities for isolation. These technical innovations enabled Robert Koch to formulate his foundational postulates for epidemiological characterization and to isolate *Mycobacterium tuberculosis* (Koch's bacillus), a breakthrough for which he was awarded the Nobel Prize in Physiology or Medicine in 1905. The laboratory's diagnostic infrastructure was further solidified in 1887 when German bacteriologist Julius Richard Petri invented the Petri dish, which remains the primary culturing platform and gold standard in diagnostic bacteriology to this day [14].

Culture media facilitate bacterial propagation and phenotypic characterization based on cellular biochemistry. Selective additives (e.g., bile salts, crystal violet) actively restrict competing non-target flora. Meanwhile, differential substrates and pH indicators provide a visual readout of enzymatic activity, differentiating isolates according to their specific carbohydrate fermentation and byproduct profiles. Sorbitol MacConkey (SMAC) agar is a differential culture medium that utilizes metabolic properties to differentiate pathogens, specifically within the species *Escherichia coli* [Fig. 2].



Figure 2: Differential Phenotypes of *Escherichia coli* on Sorbitol MacConkey (SMAC) Agar.

Note: Comparison of D-sorbitol fermentation capability on SMAC agar following incubation. **Left:** Sorbitol-fermenting bacterial culture (commensal *E. coli*) displaying intense pink-to-magenta, raised, circular colonies resulting from active acidification and neutral red indicator response. **Right:** Non-sorbitol-fermenting bacterial culture (characteristic of enterohemorrhagic *E. coli* O157:H7) producing colorless/neutral, pale colonies due to the lack of sorbitol utilization.

3 DIFFERENTIAL STAINING TECHNIQUES

In tandem with culture methods, differential staining techniques solved the critical challenge of bacterial contrast and phenotypic identification.

3.1 Gram Staining

Developed in 1884 by Danish bacteriologist Hans Christian Gram, the Gram stain became a milestone by systematically differentiating bacteria based on their cell wall ultrastructure. Gram-positive bacteria possess a thick peptidoglycan (murein) matrix composed of repeating *N*-acetylglucosamine (NAG) and *N*-acetylmuramic acid (NAM) units cross-linked by peptide bonds, whereas Gram-negative bacteria feature a thin peptidoglycan layer within the periplasmic space between an inner cytoplasmic membrane and an asymmetrical, lipopolysaccharide-rich outer membrane. Mechanistically, this four-step procedure begins with primary staining using crystal violet, a cationic dye that penetrates the cytoplasm and electrostatically binds to cellular components in both bacterial types. Next, Gram's iodine solution is added as a mordant to form a large, insoluble crystal violet-iodine (*CV-I*) complex. During decolorization with 95% ethanol or acetone, the reagent extracts lipids from the outer membrane of Gram-negative bacteria and increases its permeability to elute the *CV-I* complex, while in Gram-positive bacteria, the alcohol dehydrates the thick peptidoglycan wall, shrinking its pores and trapping the complex inside [Fig. 3]. Finally, counterstaining with safranin or basic fuchsin colors the decolorized, Gram-negative cells pink or red, while Gram-positive bacteria retain the intense initial violet stain [15].

Despite the development of advanced molecular methodologies, Gram staining remains an indispensable, highly cost-effective, and rapid diagnostic tool in clinical practice. It holds particular value in the evaluation of genitourinary conditions, including bacterial vaginosis (BV). Bacterial vaginosis is clinically defined as a complex polymicrobial dysbiosis marked by a significant reduction in dominant, hydrogen peroxide-producing *Lactobacillus* species and a concomitant proliferation of opportunistic anaerobic organisms, notably *Gardnerella vaginalis*, *Bacteroides* spp., and *Mobiluncus* spp. This disruption of physiological microflora homeostasis leads to mucosal inflammation, altered pH, and characteristic clinical symptoms such as homogeneous vaginal discharge and vulvar discomfort [12].

The standardized Nugent scoring system represents the laboratory reference standard for diagnosing bacterial vaginosis. This microscopic method quantifies specific bacterial morphotypes observed on Gram-stained vaginal smears: *Lactobacillus* morphotypes (scored 0–4), *Bacteroides*/*Gardnerella* morphotypes (scored 0–4), and curved Gram-variable rods representing *Mobiluncus* (scored 0–2). A composite score ranging from 7 to 10 is diagnostic for BV [Fig. 4]. Microscopic examination is frequently correlated with clinical criteria (Amsel's criteria), including vaginal fluid alkalinity (pH > 4.5) and positive amine odor assays [13].

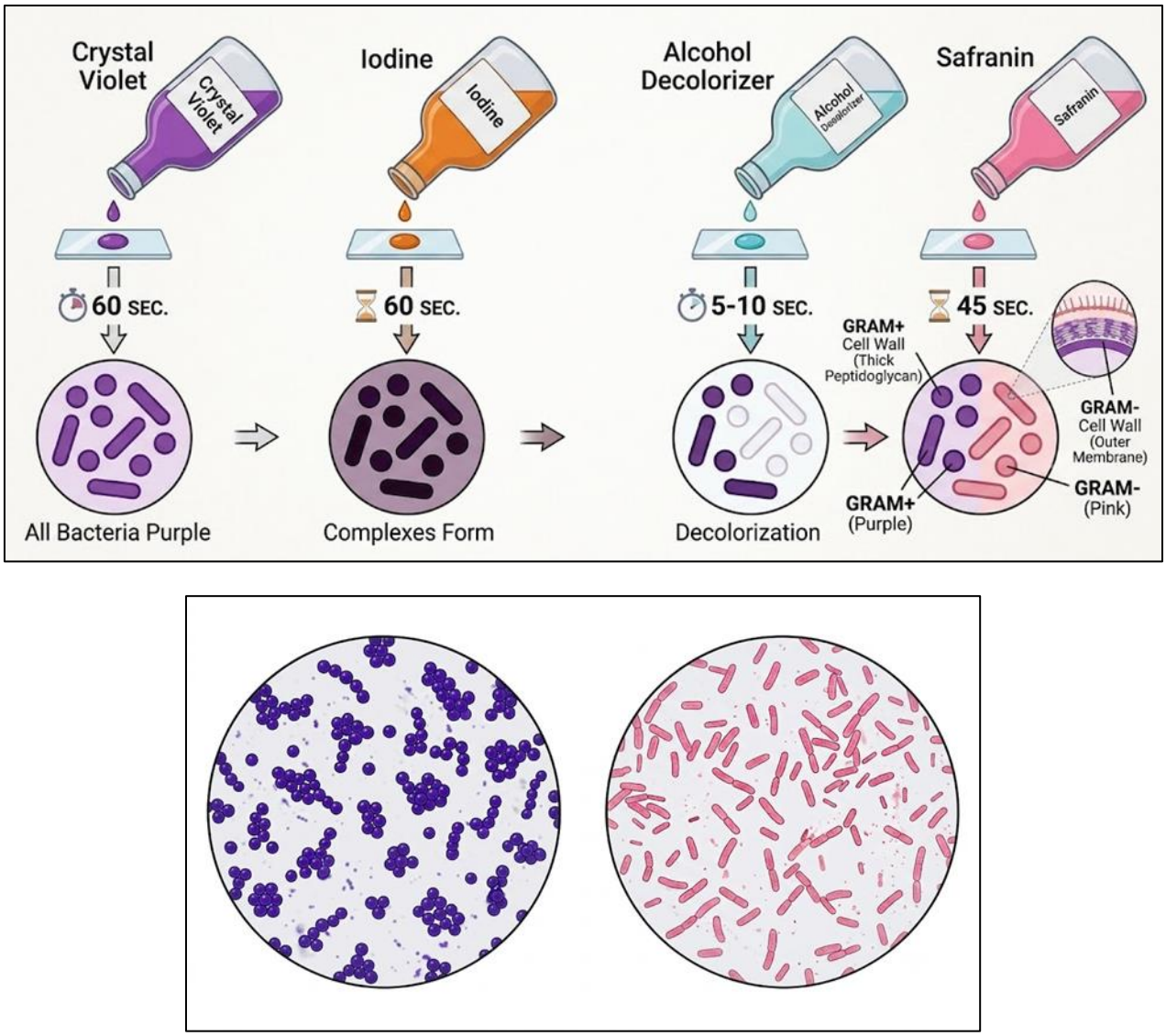


Figure 3: Microscopic Comparison of Gram-Positive and Gram-Negative Bacterial Morphology Following Gram Staining

***Notes*: Upper Figure:** Step-by-Step Gram Staining Protocol. Sequential workflow illustrating: (1) Crystal violet primary stain; (2) Iodine mordant application; (3) Ethanol/acetone decolorization; and (4) Safranin counterstain, differentiating Gram-positive (purple) from Gram-negative (pink) cells. **(Left lower) Gram-Positive Bacteria:** Demonstrates purple-stained cocci arranged in clusters and chains. The retention of the crystal violet-iodine complex is facilitated by the thick peptidoglycan layer of the Gram-positive cell wall.**(Right lower) Gram-Negative Bacteria:** Displays pink/red-stained bacilli (rods) distributed across the field. The loss of the primary stain during decolorization and subsequent counterstaining with safranin is characteristic of the thin peptidoglycan layer and outer lipid membrane.

Furthermore, microscopic examination of Gram-stained specimens is vital for differential diagnosis between bacterial vaginosis and sexually transmitted infections (STIs). For example, it enables the visualization of flagellated protozoa characteristic of *Trichomonas vaginalis* or kidney bean-shaped intracellular Gram-negative diplococci diagnostic of *Neisseria gonorrhoeae*) (Kelly, 1990). While nucleic acid amplification tests (NAATs) offer superior sensitivity, direct microscopic staining maintains clinical utility due to its immediate point-of-care feasibility and nominal operational cost [17].

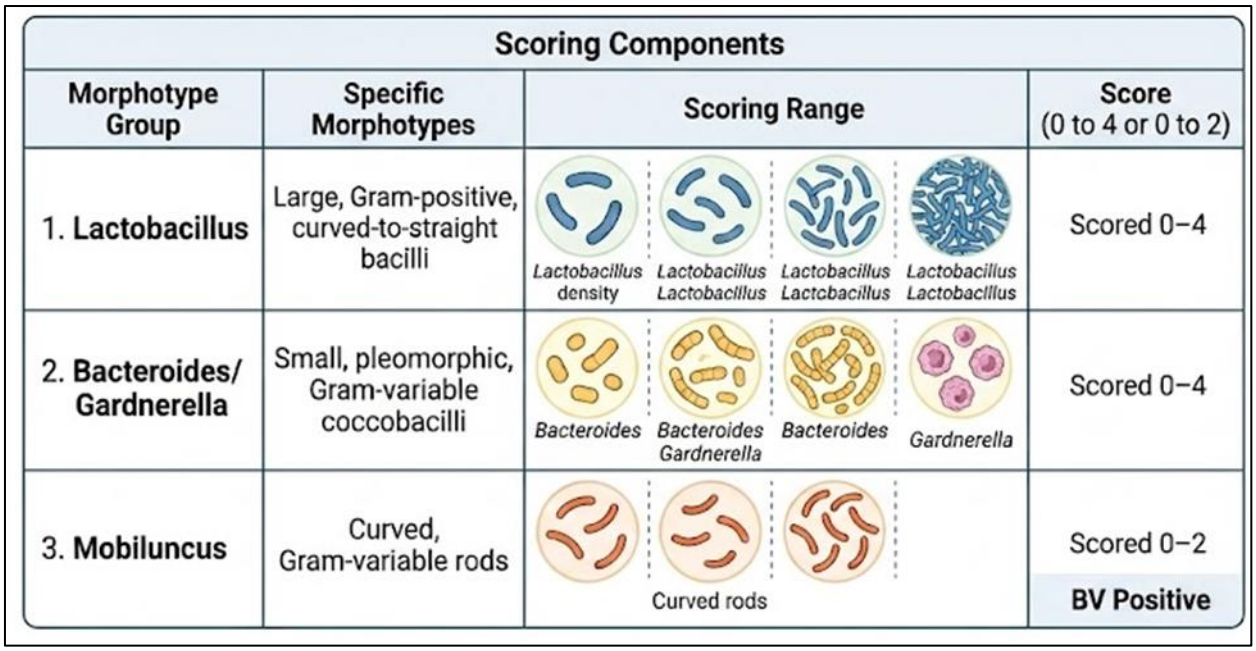


Figure 4: Overview of the Standardized Nugent Scoring System and Clinical Correlations for Bacterial Vaginosis Diagnosis

Notes: Scoring Components (Nugent System): The diagnosis is primarily based on microscopic quantification of specific bacterial morphotypes on a Gram-stained vaginal smear. **Row 1 (Lactobacillus):** Measures the density of large, Gram-positive bacilli (normal flora). A high density scores 0, while a complete absence scores 4. **Row 2 (Bacteroides/Gardnerella):** Quantifies small, pleomorphic, Gram-variable coccobacilli. A high density scores 4. **Row 3 (Mobiluncus):** Quantifies curved, Gram-variable rods. A high density scores 2. **Total Composite Score Interpretation:** The individual scores from the three categories are summed to produce a composite score (ranging 0–10). A composite score of 7–10 is strictly diagnostic for BV. **Clinical Correlation (Amsel's Criteria):** While the Nugent score is the laboratory standard, diagnosis is often correlated with physical clinical findings, specifically a vaginal fluid pH greater than 4.5 and a positive amine ("whiff") odor assay.

3.2 Acid-Fast Staining

However, conventional Gram staining presents limitations when applied to mycobacteria such as *Mycobacterium tuberculosis*, which remain refractory to the technique due to a dense, hydrophobic, and impenetrable cell wall rich in mycolic acids and waxes that repels hydrophilic dyes. To overcome this lipid barrier and facilitate dye penetration, two techniques leveraging the lipid solubility of carbolfuchsin are employed: the Ziehl-Neelsen stain, which applies direct heat to temporarily melt cell wall waxes and allow dye entry, and the Kinyoun stain (cold method), which bypasses heat by utilizing a formulation with higher concentrations of phenol and basic fuchsin [Fig. 5]. Notably, emerging evidence suggests these stains may actually target mycobacterial nucleic acids rather than binding directly to mycolic acids, with the lipid-rich cell wall instead acting to prevent decolorization a mechanistic revision of the long-held assumption described above[5]. In both methods, once carbolfuchsin crosses the cell wall, the complex resists decolorization by an acid-alcohol solution (3% HCl in 95% ethanol), a property termed acid-fastness; upon counterstaining with methylene blue, acid-fast bacilli (AFB) retain the primary dye and appear bright magenta or pink, whereas non-acid-fast organisms take up the counterstain and appear blue. Both techniques serve as frontline diagnostic tools for tuberculosis, leprosy, and other mycobacterial infections, though both are limited by insensitivity, identifying organisms in only about 20–62% of culture-positive samples depending on bacterial load and reader experience [6]. Direct comparative data indicate that Kinyoun's cold carbol-fuchsin method is inferior to both Ziehl-Neelsen and fluorochrome (auramine/auramine-rhodamine) methods when technical parameters are not tightly controlled, although sensitivity and specificity of Ziehl-Neelsen and fluorochrome methods are comparable when procedural standards are followed [7]. A large retrospective comparison of over 16,000 specimens similarly found both carbolfuchsin-based (Kinyoun) and auramine-rhodamine stains to have high specificity (>99.9%) but limited overall sensitivity (17.4%), with auramine-rhodamine favored for *M. tuberculosis* complex detection and Kinyoun retaining a modest advantage for detecting rapidly growing mycobacteria [8]. Fluorochrome-based acid-fast stains are now recognized to surpass brightfield Ziehl-Neelsen in sensitivity, particularly at low pathogen burden, and are increasingly paired with artificial intelligence-assisted slide interpretation [5]. Ziehl-Neelsen remains widely used as a frontline method for its simplicity and low cost, while Kinyoun is preferred in high-throughput laboratories to eliminate the toxic phenol vapors generated during heating [6-7].

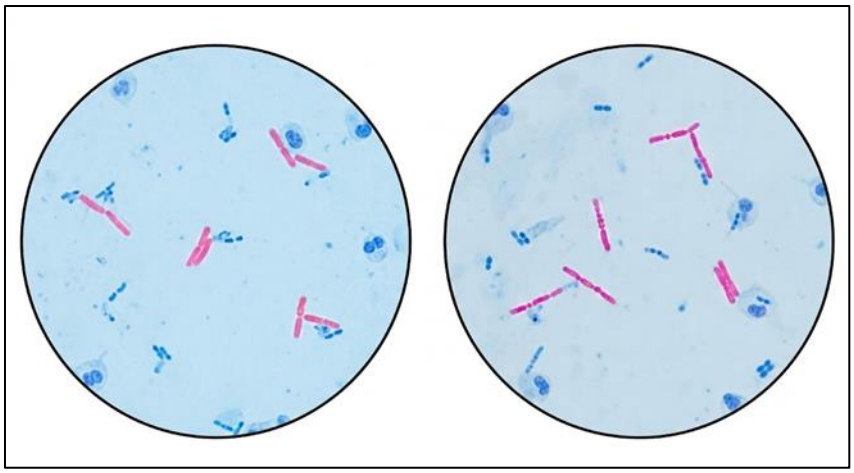


Figure : Comparison of Cold-Stain (Kinyoun) and Hot-Stain (Ziehl-Neelsen) Techniques for Acid-Fast Bacilli Differentiation

Notes: (Left) Kinyoun Stain (Cold Method): Micrograph illustrating the use of a modified carbolfuchsin stain with higher phenol concentration, which allows stain penetration without heat application. Bright fuchsia-pink, rod-shaped bacteria are clearly discernible against a light blue, non-acid-fast background. **(Right) Ziehl-Neelsen Stain (Hot Method):** Micrograph showing the traditional technique, which requires heat (steam) to facilitate the penetration of the carbolfuchsin stain through the waxy mycobacterial cell wall. Similar results are observed, with distinct pink/red AFB visible against the blue background, validating the consistency of the two staining protocols.

4 BIOCHEMICAL IDENTIFICATION AND SEROLOGY

Beyond morphological evaluation and differential staining techniques, microorganisms are dynamic biological entities that actively synthesize, reduce, and catabolize a wide array of metabolic substrates, while also possessing unique structural components that allow for their differentiation.

4.1 Serological & Fungal Diagnostics

This structural identification is particularly crucial in medical mycology, where fungi, as eukaryotic organisms, share fundamental cellular machinery with human hosts. Because eukaryotic human cells lack a cell wall entirely, the fungal cell wall represents both a defining structural differentiator and an ideal target for diagnostics and targeted therapy. Within this fungal envelope, circulating polysaccharides such as (1→3)-β-D-glucan (BDG) and galactomannan serve as essential diagnostic surrogates. Galactomannan, released during Aspergillus growth, is detectable by commercial enzyme immunoassay, with an optical density cutoff of ≥0.5–0.7 in serum (sensitivity roughly 78–92%, specificity roughly 84–91% depending on the population and cutoff used) and ≥1.0 in bronchoalveolar lavage fluid.[9][10][11] Critically, the galactomannan assay does not detect Mucorales, and BDG is likewise absent from the cell wall of Mucorales and some [9] *Cryptococcus* species, though it is present in Candida, Fusarium, and Pneumocystis [9-10]. This divergence means a negative BDG in a patient with suspected invasive aspergillosis may actually support a diagnosis of mucormycosis instead, a distinction that is clinically crucial when selecting antifungal treatment given that Mucorales are intrinsically resistant to voriconazole [10]. BDG detected via the Limulus/Tachypleus-based assay signifies fungal invasion broadly (candidiasis, fusariosis, aspergillosis, *Pneumocystis jirovecii* pneumonia) but is not specific to *Aspergillus* [11].

The catalase test, for example, differentiates staphylococci from streptococci based on the enzymatic decomposition of hydrogen peroxide into water and oxygen, a mechanism that protects bacteria from oxidative killing by host phagocytes. Similarly, the oxidase test detects the presence of bacterial cytochrome c oxidase within the electron transport chain, critically distinguishing non-fermenting Gram-negative bacilli like *Pseudomonas aeruginosa* from members of the *Enterobacteriaceae* family. Furthermore, the urease test identifies organisms capable of hydrolyzing urea into ammonia and carbon dioxide, an enzymatic activity that serves as a primary virulence factor for pathogens like *Helicobacter pylori* by enabling survival in gastric acid, and *Proteus mirabilis* by driving urinary stone formation through urine alkalinization. To streamline bacterial identification in clinical microbiology laboratories, these individual biochemical tests were miniaturized and standardized into multi-test panels, most notably the Analytical Profile Index (API) system [Fig. 6], which combines multiple dehydrated biochemical substrates, including carbohydrate fermentation, amino acid decarboxylation, and hydrogen sulfide production, into a single strip to generate a numerical profile that identifies clinically significant bacteria with high precision [18].

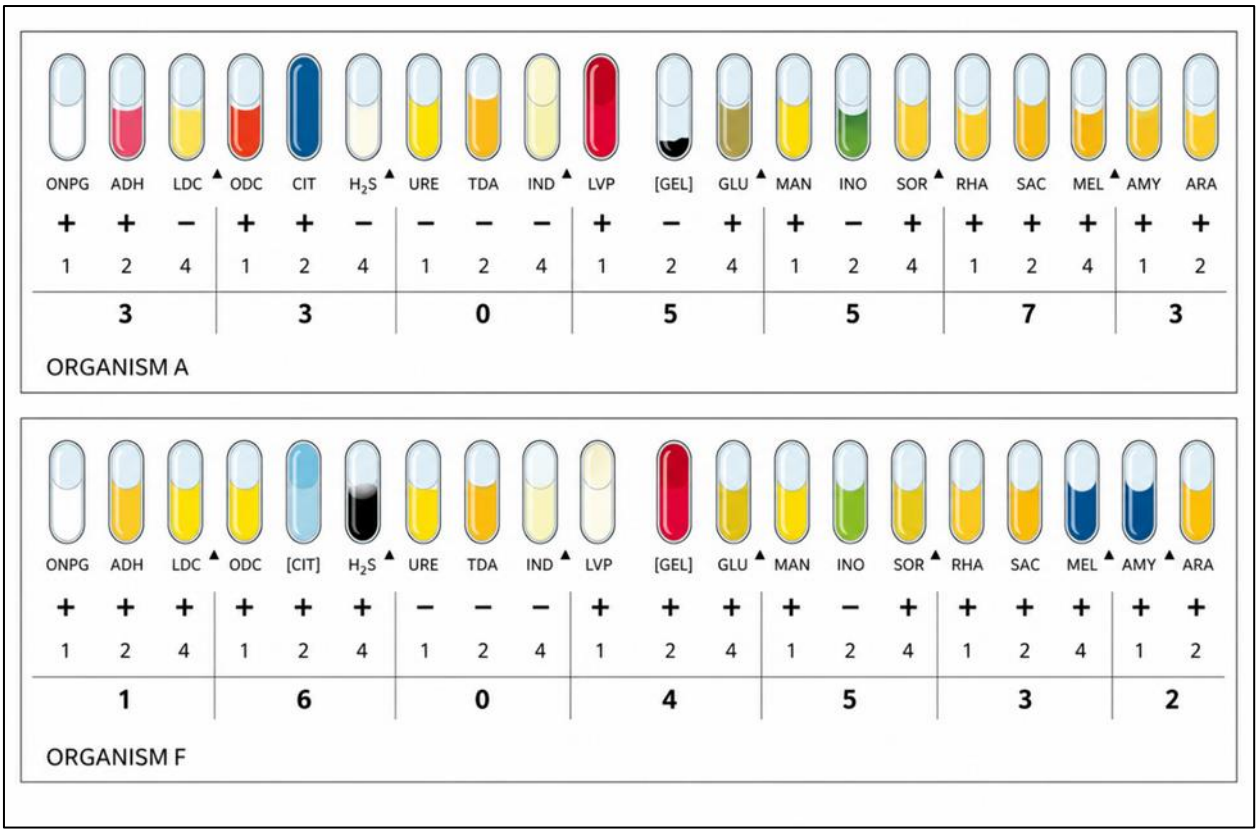


Figure 6: API 20E Biochemical Test Strips and Derived Octal Profiles for Organism A and Organism F

Notes: Colorimetric reaction profiles and numerical coding scheme obtained using the Analytical Profile Index (API 20E) system after 24 hours of incubation. Positive (+) and negative (−) biochemical reactions are grouped into triplets with positional values (1, 2, or 4) to generate a 7-digit octal code used for taxonomic identification. **Top Panel (Organism A):** Yields the octal profile **3305573**, identifying the isolate as Enterobacter cloacae with a 95.1% identification confidence. Key positive reactions include ONPG, ADH, ODC, citrate utilization (CIT), VP, and carbohydrate fermentations (GLU, MAN, SOR, RHA, SAC, MEL, AMY, ARA). **Bottom Panel (Organism F):** Yields the octal profile **1604532**, identifying the isolate as Citrobacter freundii with a 92.5% identification confidence. Characterized by positive reactions for ONPG, ADH, LDC, ODC, citrate utilization ([CIT]), hydrogen sulfide production (H_2S), gelatin hydrolysis ([GEL]), VP, and carbohydrate fermentations.

Table 1: Analytical Profile Index (API 20E) Numerical Profiles and Species Identification

Organism Reference	Generated Octal Profile	Identified Species	Identification Confidence (%)
Organism A	3305573	*Enterobacter cloacae*	95.1%
Organism F	1604532	*Citrobacter freundii*	92.5%

Note. Numerical profiles were derived from 24-hour biochemical color reaction indices evaluated against the API 20E database.

In parallel with intrinsic structural features and metabolic profiles, the interaction between the host immune system and invading pathogens provides another highly specific axis for clinical identification, relying on immunological recognition rather than microbial isolation. Serological diagnostics center on the precise molecular binding between host antibodies and specific microbial antigens, offering rapid detection of circulating pathogen-derived molecules or host-generated immune responses. Enzyme-Linked Immunosorbent Assay (ELISA) is a solid-phase immunoassay that quantifies antigens or antibodies by utilizing enzyme-conjugated reagents to produce a measurable colorimetric signal, operating through three main configurations: direct ELISA binds a conjugated primary antibody directly to an immobilized antigen for rapid detection; indirect ELISA employs an unlabeled primary antibody followed by an enzyme-linked secondary antibody to detect specific antibodies with enhanced signal amplification; and sandwich ELISA captures the target antigen between two epitope-specific antibodies, offering high specificity for complex samples. Complementing these enzyme-based methods, indirect immunofluorescence (IFI) uses fluorophore-tagged secondary antibodies to visualize bound primary antibodies under a fluorescence microscope, enabling simultaneous quantitative detection and spatial localization of target antigens or antibodies in cellular and tissue preparations [19].

In contrast to antibody-mediated humoral assays, other diagnostic modalities capitalize on specialized cell-mediated immune cascades to identify pathogens that evade humoral detection or establish latent intracellular infections. A primary example of this cellular approach is the Interferon-Gamma Release Assay (IGRA), used in the diagnosis of

Mycobacterium tuberculosis. Instead of detecting circulating antibodies, which often fail to differentiate active from latent tuberculosis or cross-react with non-tuberculous mycobacteria, IGRA measures the specific release of interferon-gamma by memory T-lymphocytes upon ex vivo exposure to specific *M. tuberculosis* antigens, such as ESAT-6 and CFP-10. Thus, while humoral immunoassays detect antigen-antibody complexes directly, cell-mediated assays like IGRA exploit the memory and signaling cascades of host effector cells to confirm exposure with high diagnostic specificity [20].

Immunodiagnostic serotyping provides targeted pathogen detection via specific antigen-antibody binding. Utilizing antibody-functionalized magnetic Dynabeads, microscopic evaluation revealed distinct physical distribution patterns between strains [Fig. 7]. Non-pathogenic *E. coli* K-12 displayed a homogeneous, unaggregated cellular dispersion, confirming the lack of target O157:H7 surface antigens. Conversely, the pathogenic serotype *E. coli* O157:H7 formed prominent, cross-linked agglutination complexes, confirming positive binding [21].

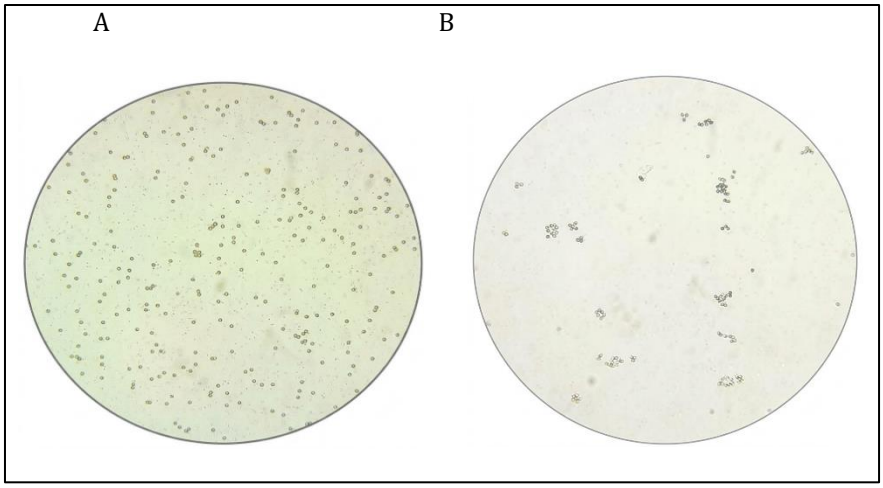


Figure 7: Microscopic optical fields illustrating the physical distribution patterns of antibody-functionalized magnetic Dynabeads when exposed to non-pathogenic and pathogenic bacterial strains.

Note: (A) Non-Pathogenic Control (*E. coli* K-12): Displays a homogeneous, unaggregated cellular dispersion across the field of view, confirming the absence of target O157:H7 surface antigens and negative binding. **(B) Target Pathogen (*E. coli* O157:H7):** Exhibits prominent, irregular cross-linked agglutination complexes, validating positive antibody-antigen binding and successful immunodiagnostic serotyping.

5 MOLECULAR DIAGNOSTICS & 16S RRNA PHYLOGENETICS

Advancing beyond immunological recognition and phenotype-based testing, modern microbiological diagnostics have expanded into the molecular architecture of the microbial genome. Rather than relying solely on phenotypic traits, modern assays identify pathogens through their primary genetic sequence: deoxyribonucleic acid (DNA) and ribonucleic acid (RNA). Molecular diagnostic techniques typically begin with the polymerase chain reaction (PCR), which selectively amplifies target nucleotide sequences composed of purine and pyrimidine bases. These nitrogenous bases form complementary hydrogen bonds that predictably denature and anneal at specific thermal thresholds during amplification cycles. Following amplification, the physical properties of these nucleic acid fragments can be evaluated using agarose gel electrophoresis. When exposed to an electric field within a porous hydrogel matrix, negatively charged nucleic acids migrate toward the anode at rates inversely proportional to the logarithm of their molecular weight, causing larger fragments to migrate slowly while smaller fragments travel further through the gel. Beyond size determination, precise taxonomic identification relies on target nucleic acid sequencing. Rather than sequencing the entire genome, clinical diagnostics often target highly conserved phylogenetic marker genes that function as molecular fingerprints, most notably the 16S ribosomal RNA (16S rRNA) gene in bacteria. By sequencing hypervariable regions within the 16S rRNA gene and aligning them against curated reference databases, comparative phylogenetics can precisely delineate bacterial species, providing definitive identification even for fastidious or unculturable organisms [22].

16S ribosomal RNA (rRNA) gene sequencing serves as the gold standard molecular tool for bacterial taxonomy and evolutionary classification due to its highly conserved and variable region architecture [Fig. 8]. Phylogenetic tree reconstruction based on 16S rRNA gene alignments revealed distinct evolutionary clustering among the analyzed isolates. *Citrobacter freundii* (Organism F) and *Enterobacter cloacae* (Organism A) exhibited close phylogenetic proximity within the tree topology, consistent with their shared facultatively anaerobic, Gram-negative enterobacterial lineage. Conversely, *Pseudomonas aeruginosa* (Organism B) formed a well-supported outgroup at a substantial

evolutionary distance from the Enterobacteriaceae clade, reflecting its obligate/strict aerobic respiratory metabolism and fundamental taxonomic divergence [23].

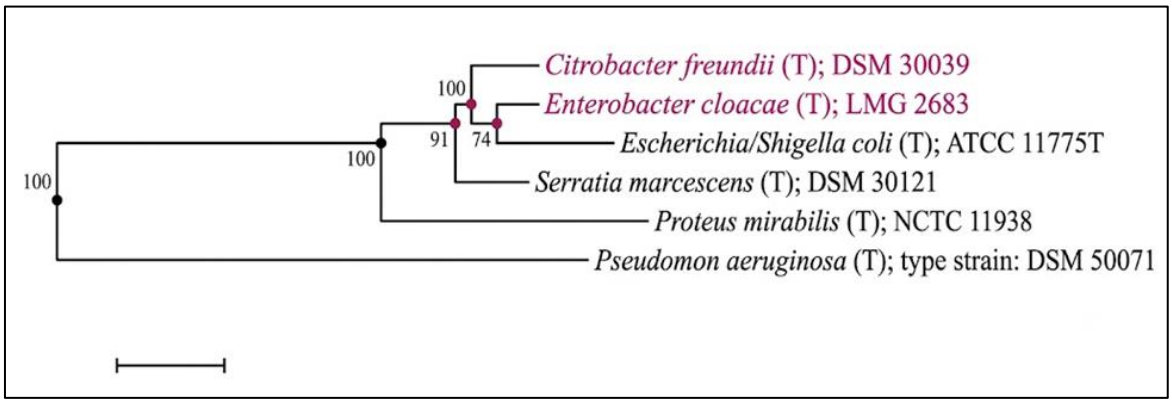


Figure 8: Molecular Phylogenetic Reconstruction of 16S rRNA Gene Sequences Showing Evolutionary Relationships Among Enterobacteriaceae Isolates and Outgroup Strains

Notes: Dendrogram constructed from 16S rRNA gene sequence alignments demonstrating evolutionary clustering and topological placement. Numbers at internal nodes represent bootstrap support values (%) derived from resampling analysis. **Target Isolates (Highlighted in Magenta):** *Citrobacter freundii* (DSM 30039) and *Enterobacter cloacae* (LMG 2683) form a highly supported clade (100% bootstrap confidence), confirming their high degree of genetic identity and shared lineage within the Enterobacteriaceae family. **Enteric Clade Relations:** The *C. freundii–E. cloacae* cluster shares a sister clade relationship with *Escherichia/Shigella coli* (74% bootstrap value) and nests alongside other enterobacteria, including *Serratia marcescens* (91% bootstrap support) and *Proteus mirabilis*. **Outgroup Rooting:** *Pseudomonas aeruginosa* (DSM 50071) resolves as a distinct, basal outgroup rooted with 100% bootstrap support, illustrating significant sequence divergence consistent with its non-enteric taxonomic classification.

Table 2: Comparative 16S rRNA Gene Sequence Alignment Scores (seqmatch) Across Isolates A–F

Organism Reference	Sequence Match Identification	seqmatch Score (S_ab)
Organism A	*Enterobacter cloacae*	1.000
Organism B	*Pseudomonas aeruginosa*	1.000
Organism C	*Escherichia/Shigella coli*	1.000
Organism D	*Serratia marcescens*	0.939
Organism E	*Proteus mirabilis*	0.980
Organism F	*Citrobacter freundii*	1.000

Note. Sequence similarity matching score (S_ab) of 1.000 denotes perfect sequence identity across the amplified genomic region.

6 CONCLUSION

This study traces the evolution of diagnostic microbiology from empirical microscopy to advanced molecular profiling, demonstrating that while sophisticated methods enable direct pathogen identification, foundational techniques retain enduring clinical utility. Integrating classical phenotypic assays with high-resolution genomic tools establishes an optimal diagnostic framework. Ultimately, this approach benefits society by accelerating targeted therapy, curbing resistant infections, and strengthening public health surveillance.

STATEMENTS ON COMPLIANCE WITH ETHICAL STANDARDS

Acknowledgments

The authors gratefully acknowledge the institutional support provided by the Pontificia Universidad Católica del Ecuador and the collaborative technical resources that facilitated the compilation of this historical and methodological review.

Disclosure of conflict of interest

The authors declare no conflicts of interest regarding this manuscript.

REFERENCES

[1] Foster BL. On the discovery of cementum. *Journal of Periodontal Research*. 2017;52(4):666-685. doi:10.1111/jre.12444.

[2] Cocquyt T, Zhou Z, Plomp J, van Eijck L. Neutron Tomography of Van Leeuwenhoek's Microscopes. *Science Advances*. 2021;7(20):eabf2402. doi:10.1126/sciadv.abf2402.

[3] Kutschera U. Antonie Van Leeuwenhoek (1632-1723): Master of Fleas and Father of Microbiology. *Microorganisms*. 2023;11(8):1994. doi:10.3390/microorganisms11081994.

[4] Lane N. The Unseen World: Reflections on Leeuwenhoek (1677) 'Concerning Little Animals'. *Philosophical Transactions of the Royal Society of London. Series B, Biological Sciences*. 2015;370(1666):20140344. doi:10.1098/rstb.2014.0344.

[5] Hänscheid T, Mahomed S, Oliveira L, Pereira DS, Grobusch MP. Fluorescent Acid-Fast Stains for Diagnosing Mycobacteria and Beyond: Back to the Future?. *The Lancet. Microbe*. 2025;:101233. doi:10.1016/j.lanmic.2025.101233.

[6] Michelow P, Omar T, Field A, Wright C. The cytopathology of mycobacterial infection. *Diagnostic Cytopathology*. 2016;44(3):255-62. doi:10.1002/dc.23410.

[7] Somoskövi A, Hotaling JE, Fitzgerald M, et al. Lessons From a Proficiency Testing Event for Acid-Fast Microscopy. *Chest*. 2001;120(1):250-7. doi:10.1378/chest.120.1.250.

[8] Mahmud HA, She RC. Comparison of Diagnostic Accuracy and Sensitivity of Kinyoun and Auramine-Rhodamine Stains in Detecting Mycobacteria From Specimen Smears. *Microbiology Spectrum*. 2026;14(7):e0047526. doi:10.1128/spectrum.00475-26.

[9] European Society for Blood and Marrow Transplantation. The manual of choice for doctors and practitioners involved in Hematopoietic Cell Transplantation (HCT) and Cellular Therapies. 2024.

[10] Schelenz S, Abdolrasouli A, Armstrong-James D, et al. British Society for Medical Mycology Best Practice Recommendations for the Diagnosis of Serious Fungal Diseases: 2025 Update. *The Lancet. Infectious Diseases*. 2025;:S1473-3099(25)00550-X. doi:10.1016/S1473-3099(25)00550-X.

[11] Patterson TF, Thompson GR, Denning DW, et al. Practice Guidelines for the Diagnosis and Management of Aspergillosis: 2016 Update by the Infectious Diseases Society of America. *Clinical Infectious Diseases : An Official Publication of the Infectious Diseases Society of America*. 2016;63(4):e1-e60. doi:10.1093/cid/ciw326.

[12] Mondal, A.S., Sharma, R. and Trivedi, N. (2023) 'Bacterial vaginosis: A state of microbial dysbiosis', *Medicine in Microecology*, 16, p. 100082. doi:10.1016/j.medmic.2023.100082.

[13] Mohammadzadeh, F. *et al.* (2014) 'Diagnostic value of Amsel's clinical criteria for diagnosis of bacterial vaginosis', *Global Journal of Health Science*, 7(3). doi:10.5539/gjhs.v7n3p8.

[14] Basu, S. *et al.* (2015) 'Evolution of bacterial and Fungal Growth Media', *Bioinformation*, 11(4), pp. 182–184. doi:10.6026/97320630011182.

[15] Rohde, M. (2019) 'The gram-positive bacterial cell wall', *Microbiology Spectrum*, 7(3). doi:10.1128/microbiolspec.gpp3-0044-2018.

[16] Masters, B.R. (2008) 'History of the optical microscope in Cell Biology and medicine', *Encyclopedia of Life Sciences* [Preprint]. doi:10.1002/9780470015902.a0003082.

[17] Kusumadewi, Y.P. *et al.* (2025) 'Gram stain evaluation in Dermatovenereology Clinic and Microbiology Laboratories: Case series', *Journal of Clinical Microbiology and Infectious Diseases*, 5(1), pp. 1–5. doi:10.51559/jcmid.v5i1.59.

[18] Iwase, T. *et al.* (2013a) 'A simple assay for measuring catalase activity: A visual approach', *Scientific Reports*, 3(1). doi:10.1038/srep03081.

[19] Hornbeck, P., Winston, S.E. and Fuller, S.A. (1991) 'Enzyme-linked immunosorbent assays (elisa)', *Current Protocols in Molecular Biology*, 15(1). doi:10.1002/0471142727.mb1102s15.

[20] Trajman, A., Steffen, R.E. and Menzies, D. (2013) 'Interferon-gamma release assays versus tuberculin skin testing for the diagnosis of latent tuberculosis infection: An overview of the evidence', *Pulmonary Medicine*, 2013, pp. 1–11. doi:10.1155/2013/601737.

[21] Gheorghiu, E. (2021) 'Detection of pathogenic bacteria by Magneto-immunoassays: A review', *The Journal of Biomedical Research*, 35(4), p. 277. doi:10.7555/jbr.34.20200123.

[22] Gajic, I. *et al.* (2026) 'Evolving approaches to bacterial identification: A review of classical and modern techniques', *International Journal of Molecular Sciences*, 27(11), p. 5092. doi:10.3390/ijms27115092.